# Lost Heat Capacity and Entropy in the Helical Magnet MnSi

Sergei M. Stishov,[1,*] Alla E. Petrova,[1] Anatoly A. Shikov,[2] Thomas A. Lograsso,[3] Eyvaz I. Isaev,[4] Börje Johansson,[5] and Luke L. Daemen[6]

[1]*Institute for High Pressure Physics of Russian Academy of Sciences, Troitsk, Moscow Region, Russia*
[2]*Russian Research Center Kurchatov Institute, Moscow 123182, Russia*
[3]*Ames Laboratory, Iowa State University, Ames, Iowa 50011, USA*
[4]*Department of Physics, Chemistry and Biology, SE-581 83, Linkoping University, Sweden*
[5]*Applied Materials Physics, Materials Science Department, The Royal Technological University, SE-100 44 Stockholm, Sweden*
[6]*Los Alamos National Laboratory, Los Alamos, New Mexico 87545, USA*

(Received 28 September 2010; published 2 December 2010)

The heat capacity of MnSi at $B = 0$ and $B = 4$ T was measured in the temperature range 2.5–100 K. To analyze the data, calculations of the phonon spectrum and phonon density of states in MnSi were performed. The calculated phonon frequencies were confirmed by means of inelastic neutron scattering. The analysis of the data suggests the existence of negative contributions to the heat capacity and entropy of MnSi at $T > T_c$ that may imply a specific ordering in the spin subsystem in the paramagnetic phase of MnSi.

DOI: 10.1103/PhysRevLett.105.236403 PACS numbers: 71.27.+a, 63.20.D−, 75.40.Cx

The itinerant helical magnet MnSi has been extensively studied for a number of decades. Magnetic ordering at about 30 K in MnSi was found in Ref. [1]. The helical magnetic structure of MnSi was established in Ref. [2]. The first measurements of the heat capacity of MnSi at a modest resolution were carried out by Fawcett, Maita, and Wernick [3] and showed a simple peak, which was interpreted as evidence of a second-order phase transition in MnSi. Since then, this interpretation has been taken for granted in the literature in spite of strong evidence in favor of a first-order phase transition [4,5]. However, recent studies of the heat capacity, thermal expansion, resistivity, and elastic properties of a high quality single crystal of MnSi exposed first-order features of the phase transition [6–8]. These studies revealed the existence of unexplained aspects of the phase transition, such as maxima or minima of the heat capacity, thermal expansion coefficient, and resistivity temperature coefficient on the high-temperature side of the corresponding peaks (see also [9–11]). Recently, the formation of a Skyrmion-like spin texture was suggested to explain the above-mentioned features of the phase transition in MnSi [12]. This idea has found support at the interpretation of a neutron scattering experiment in Ref. [13]. The Skyrmion hypothesis appeared very relevant given the identification of Skyrmion crystals in the so-called $A$ phases of MnSi and $Fe_{1-x}Co_xSi$ [14–16]. The real-space observation of a Skyrmion crystal in $Fe_{1-x}Co_xSi$ leaves little doubt that a Skyrmion lattice may be formed in itinerant magnets without inversion symmetry [16]. Yet it is unclear whether there is a link between these findings and the existence of a Skyrmion liquid at zero magnetic field at $T > T_c$ in MnSi. The Skyrmion idea [12,13] was heavily disputed in Ref. [17]. The authors of Ref. [17] believe that the small angle neutron scattering data at $T > T_c$ in MnSi (see also Refs. [18–20]) are well described in the model of three regimes of critical fluctuations corresponding to the Bak-Jensen hierarchy of interactions [5]. It is clear, therefore, that the MnSi saga is not complete yet, and much remains to be done to understand fully this intriguing material.

In the present work, we report results of new measurements and analysis of the heat capacity of MnSi. The measurements included data collection at a magnetic field of 4 T, which suppresses strongly the longitudinal spin fluctuations and the phase transition. To analyze the experimental data, calculations of the phonon spectrum and phonon density of states in MnSi were performed. Inelastic neutron scattering with a polycrystalline sample of MnSi was used to validate the computational results. The combination of the experimental and theoretical data turned out to be decisive in revealing some hidden features of the thermal excitations in MnSi. In particular, the analysis of the available data led conclusively to the existence of a negative contribution to the heat capacity and entropy in MnSi at $T > T_c$, implying that a specific spin ordering process did occur in the paramagnet phase of MnSi. The heat capacity of a MnSi single crystal [21] was measured with an adiabatic vacuum calorimeter by the heat pulse method in the temperature range 2–100 K. The measurements in magnetic fields were carried out with a superconducting solenoid magnet. The magnetic field was oriented along the [110] direction of the single crystal. The overall accuracy of the heat capacity measurements was approximately 1%–1.5%. Some of the data in the range 2–40 K have been published earlier in Refs. [6,7]. In the present Letter, we extend the measurements to 100 K. These results were crucial for the analysis of the heat capacity of MnSi at $T > T_c$. At the same time, an

 

effective analysis of the data would not be possible without the extended calculations of the phonon spectra of MnSi. Some details of the calculations are described below.

Static total energy calculations were performed within the framework of the spin-polarized version of the density functional theory [22] to obtain a fully relaxed structure [23], including equilibrium lattice parameter and atomic positions for Mn and Si. To calculate the phonon dispersion relations in MnSi, we used the linear response method implemented in the QUANTUM ESPRESSO code [24]. Electron-ion interactions were described by means of ultrasoft pseudopotentials [25], and the exchange-correlation effects were treated in the framework of the generalized gradient approximation [26]. Plane waves with a maximum kinetic energy of 40 Ry were used in the expansion of the electron wave functions in the periodic crystal, and plane waves with a maximum kinetic energy of 480 Ry were used to describe the augmented charge. Integration over the Brillouin zone was performed by using an $8 \times 8 \times 8$ $k$-mesh grid. The self-consistent threshold was accepted at $10^{-10}$ Ry for structure optimization and $10^{-14}$ Ry for phonon calculations. Phonon dispersion relations were calculated by using the real-space force constants matrix obtained via fast Fourier transformation of 11 dynamical matrices. The phonon density of states (PhDOS) and thermodynamic properties of the silicides were calculated by using the QHA code [27]. The calculated lattice parameter 4.5476 Å is in excellent agreement with the experimental lattice parameter 4.549 Å extrapolated to zero temperature [7,28,29]. The atomic parameters for Mn, $u_{\mathrm{Mn}} = 0.1374$, and for Si, $u_{\mathrm{Si}} = 0.8451$, also matched perfectly the available experimental data: $u_{\mathrm{Mn}} = 0.138$ [28] and 0.137 [30] and $u_{\mathrm{Si}} = 0.845$ [28] and 0.846 [30]. The calculated values of sound velocities and elastic constants of MnSi were found to be in good agreement with the experimental data (see Table I). The phonon contributions to the heat capacity and entropy of MnSi can be readily calculated by using the obtained PhDOS (Fig. 1). Actually, our calculations yield $C_v$, which is used to analyze the experimental $C_p$ data. However, the estimates show that the value of $C_p - C_v$ is at most 0.1 J/mol K in the studied temperature range. This difference is small enough that it does not affect our conclusions. A calculated low-temperature value of the effective Debye temperature (664 K) matches very well the experimental value (660 K) obtained from the elastic properties of MnSi [31]. It is worth noting that calculations of the PhDOS in the nonmagnetic B20 state of MnSi shows some influence of magnetic ordering on the phonon heat capacity of MnSi, but this does not change the essence of the forthcoming analysis. A verification of the calculated PhDOS was made by means of neutron scattering with a MnSi polycrystalline powder on the Filter Difference Spectrometer at Los Alamos National Laboratory. The MnSi sample was placed in a cylindrical aluminum sample holder approximately 15 mm in diameter and 100 mm tall. The sample holder was sealed under helium to provide thermal conductivity at low temperature. The sample was then placed in a top-loading, closed-cycle refrigerator and cooled to 10 K over a period of 2 hours. Data were collected for approximately 16 hours (neutron energy loss), and the raw spectrum was deconvoluted numerically with the instrumental resolution function. Because of instrument configuration, an average over all points in the Brillouin zone automatically takes place. There are no selection rules for neutron-nucleus scattering. All vibrational modes contribute to the phonon density of states. The energy transfer scale is calibrated at the beginning of each run cycle, which results in an uncertainty on peak positions of less than 5 $\mathrm{cm}^{-1}$. Mn and Si have comparable total neutron scattering cross sections, but the absorption cross section of Mn is significantly larger than that of Si. This affects the relative intensities but not the position of the phonon modes. It follows that the computed density of states will display features comparable to the experimental spectrum in terms of peak positions, but a direct comparison of peak intensities is not possible. Figure 1 displays the experimental vibrational spectrum of the MnSi polycrystal, as well as the calculated PhDOS. Note that the width of the experimental peaks corresponds to the instrumental resolution. As one can see, the positions of the phonon peaks in Figs. 1(a) and 1(b) agree to better than 10 $\mathrm{cm}^{-1}$. This encouraging result validates our calculation of the phonon contribution to the heat capacity of MnSi. The results of measurements and calculations of the heat capacity of MnSi are displayed in Fig. 2. As can be

TABLE I. Calculated sound velocities and elastic constants of MnSi compared with experimental data taken at 4 K [31] shown in parentheses.

| Sound velocity, km/s | Elastic constants, GPa |
|---|---|
| $v[100]^{L} = 7.6$ (7.4) | $C_{11} = 340$ (321) |
| $v[100]^{T2} = 4.3$ (4.64) | $C_{44} = 108$ (126) |
| $v[110]^{T2} = 4.5$ (4.47) | $C_{11} - C_{12} = 237$ (234) |

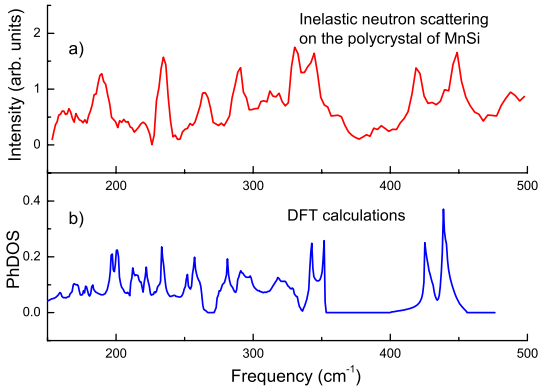


FIG. 1 (color online). Phonon density of states in MnSi: (a) neutron scattering data—no corrections for different cross sections and absorptions were made; (b) calculations—see text.

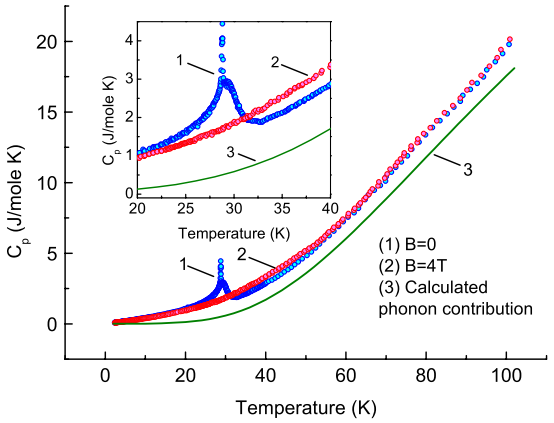


FIG. 2 (color online). The experimental heat capacity of MnSi at $B = 0$ (1) and $B = 4$ T (2) and the calculated phonon contribution (3).

seen, the heat capacity of MnSi at $B = 4$ T is always higher than that at $B = 0$ at $T > T_c$ (see also Fig. 3). In this connection we recall that a magnetic field suppresses the spin fluctuations [32]. Since the heat capacity in MnSi increases upon application of a magnetic field, one may conclude that the well-developed spin fluctuations in MnSi at $T > T_c$ and $B = 0$ provide a negative contribution to the heat capacity of MnSi above $T_c$ (see [33–36]). Turning again to Fig. 2, one can compare the experimental data with the calculation to get an idea of the magnitude of the magnetic contribution to the total heat capacity of MnSi. Upon subtraction of the phonon contribution from the heat capacity of MnSi at $B = 0$ and $B = 4$ T (Fig. 3), we see that the impressive growth of $C_p$ with temperature displayed in Fig. 2 has a nonphonon origin at $T < T_c$ but is almost completely due to phonons at $T > T_c$. A quasilinear behavior of $\Delta C_p = (C_p - C_{\rm ph})$ at $B = 4$ T most probably reflects the dominant role of the linear electronic term $\gamma T$ with $\gamma = 0.032$ J/mol K$^2$ (Ref. [7]). When $B = 0$, a spin fluctuation contribution is the most distinctive part of the heat capacity curve at $T < T_c$. Next we present the dependence of the ratio $\Delta C_p/T$ ($B = 0$) on temperature (Fig. 4). This ratio is of prime significance for the problem under consideration. As can be seen, the extrapolation of the high-temperature branch of $\Delta C_p/T$ ($B = 0$) to $T = 0$ clearly reveals the existence of a linear term in the heat capacity at $T > T_c$ with practically the same $\gamma$ as at $T < T_c$ (Ref. [7]). Upon subtracting the linear electronic term 0.036 T J/(mol K) from the heat capacity $\Delta C_p$ and from the entropy term $\Delta S$ (both deprived of their phonon contribution), one gets the results displayed in Fig. 5. These results show unambiguously negative contributions to the heat capacity and entropy of MnSi at $T > T_c$. This peculiar behavior of the heat capacity and entropy in itinerant magnetic systems was predicted many years ago in Ref. [33] (see also [34–36]) as a consequence of nonlinear effects in a fluctuating spin subsystem (mode-mode interaction). The present experimental data completely support this deduction and provide a certain link to the Skyrmion idea because a decreased entropy implies some sort of ordering, which in the given case is related to the spin subsystem.

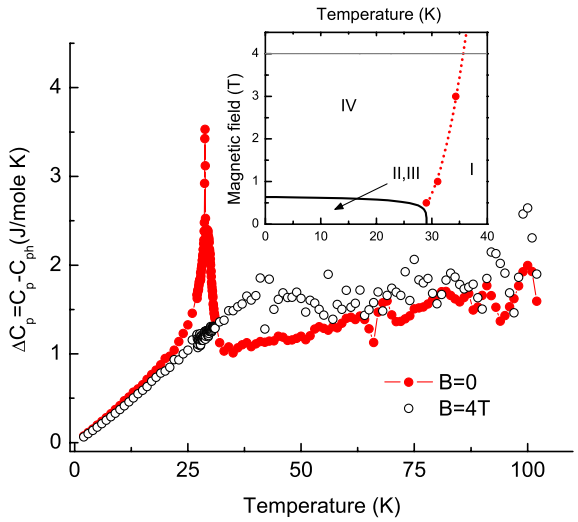


FIG. 3 (color online). The heat capacity of MnSi $\Delta C_p = C_p - C_{\rm ph}$ at zero field and at 4 T minus the phonon contributions. The partial magnetic phase diagram is shown in the inset. (I) Paramagnetic phase; (II),(III) helical and conical phases; (IV) field-induced ferromagnetic phase; dotted line—minima of the thermal expansion coefficient of MnSi [7].

In conclusion, we have measured the heat capacity of MnSi at $B = 0$ and $B = 4$ T in the temperature range 2.5–100 K. The phonon frequencies in MnSi were determined with inelastic neutron scattering. Calculations of the phonon spectrum and phonon density of states were performed, with results in good agreement with the available experimental data. The analysis of the data suggests the existence of negative contributions to the heat capacity and entropy of MnSi at $T > T_c$, in agreement with the theoretical prediction [33]. This result may be related to a

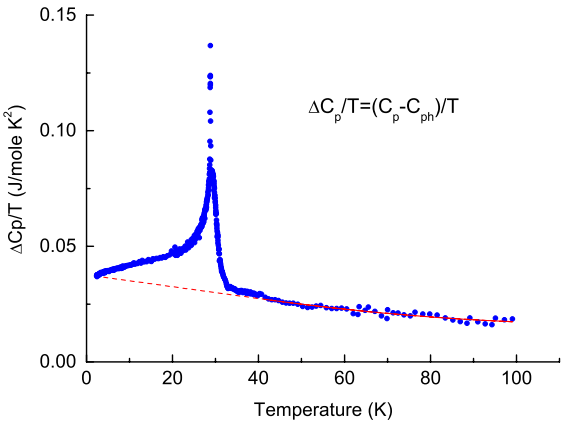


FIG. 4 (color online). The linear heat capacity term at $T > T_c$ in MnSi in zero field is the same as that at $T < T_c$.

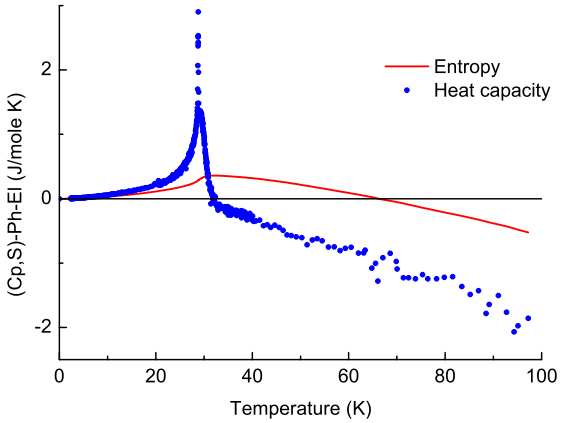


FIG. 5 (color online). The heat capacity and entropy of MnSi minus the phonon and linear electron parts. Negative partial contributions in both are apparent.

specific ordering in the spin subsystem of the paramagnetic phase of MnSi. Whether this ''ordering'' indicates a tendency toward the formation of a Skyrmion-like texture or whether it just reflects a spin localization effect remains to be seen. The evolution of the heat capacity negative term along the phase transition line at $T \rightarrow 0$ may be of primary interest to understand the peculiar properties of the paramagnetic phase of MnSi at low temperatures and high pressures.

S. M. S. and A. E. P. appreciate support of the RFBR and Program of RAS on Strongly Correlated Systems. T. A. L. acknowledges research performed at the Ames Laboratory. E. I. I. thanks the SSF, MS2E, Goran Gustafsson Foundation, and RFBR for financial support. This work has benefited from the use of the Manuel Lujan, Jr. Neutron Scattering Center (LANL).

*sergei@hppi.troitsk.ru

[1] H. J. Williams, J. H. Wernick, R. C. Sherwood, and G. K. Wertheim, J. Appl. Phys. **37**, 1256 (1966).
[2] Y. Ishikawa, K. Tajima, D. Bloch, and M. Roth, Solid State Commun. **19**, 525 (1976).
[3] E. Fawcett, J. P. Maita, and J. H. Wernick, Int. J. Magn. **1**, 29 (1970).
[4] Y. Ishikawa, T. Komatsubara, and D. Bloch, Physica (Amsterdam) **86B–88B**, 401 (1977).
[5] P. Bak and M. H. Jensen, J. Phys. C **13**, L881 (1980).
[6] S. M. Stishov, A. E. Petrova, S. Khasanov, G. Kh. Panova, A. A. Shikov, J. C. Lashley, D. Wu, and T. A. Lograsso, Phys. Rev. B **76**, 052405 (2007).
[7] S. M. Stishov, A. E. Petrova, S. Khasanov, G. Kh. Panova, A. A. Shikov, J. C. Lashley, D. Wu, and T. A. Lograsso, J. Phys. Condens. Matter **20**, 235222 (2008).
[8] A. E. Petrova and S. M. Stishov, J. Phys. Condens. Matter **21**, 196001 (2009).
[9] S. Kusaka, K. Yamamoto, T. Komatsubara, and Y. Ishikawa, Solid State Commun. **20**, 925 (1976).
[10] M. Matsunaga, Y. Ishikawa, and T. Nakajima, J. Phys. Soc. Jpn. **51**, 1153 (1982).
[11] C. Pfleiderer, J. Magn. Magn. Mater. **226–230**, 23 (2001).
[12] U. K. Rößler, A. N. Bogdanov, and C. Pfleiderer, Nature (London) **442**, 797 (2006).
[13] C. Pappas, E. Leliévre-Berna, P. Falus, P. M. Bentley, E. Moskvin, S. Grigoriev, P. Fouquet, and B. Farago, Phys. Rev. Lett. **102**, 197202 (2009).
[14] S. Mühlbauer, B. Binz, F. Jonietz, C. Pfleiderer, A. Rosch, A. Neubauer, R. Georgii, and P. Böni, Science **323**, 915 (2009).
[15] W. Münzer, A. Neubauer, T. Adams, S. Mühlbauer, C. Franz, F. Jonietz, R. Georgii, P. Böni, P. Pedersen, M. Schmidt, A. Rosch, and C. Pfleiderer, Phys. Rev. B **81**, 041203(R) (2010).
[16] X. Z. Yu, Y. Onose, N. Kanazawa, J. H. Park, J. H. Han, Y. Matsui, N. Nagaosa, and Y. Tokura, Nature (London) **465**, 901 (2010).
[17] S. V. Grigoriev, S. V. Maleyev, E. V. Moskvin, V. A. Dyadkin, P. Fouquet, and H. Eckerlebe, Phys. Rev. B **81**, 144413 (2010).
[18] Y. Ishikawa and M. Arai, J. Phys. Soc. Jpn. **53**, 2726 (1984).
[19] B. Lebech, J. Bernhard, and T. Freltoft, J. Phys. Condens. Matter **1**, 6105 (1989).
[20] S. V. Grigoriev, S. V. Maleyev, A. I. Okorokov, Yu. O. Chetverikov, R. Georgii, P. Böni, D. Lamago, H. Eckerlebe, and K. Pranzas, Phys. Rev. B **72**, 134420 (2005).
[21] Single crystal of MnSi was grown by the Bridgman technique at the Ames Laboratory and characterized in Refs. [6–8].
[22] P. Hohenberg and W. Kohn, Phys. Rev. **136**, B864 (1964); W. Kohn and L. J. Sham, Phys. Rev. **140**, A1133 (1965).
[23] R. Wentzkovich, Phys. Rev. B **44**, 2358 (1991).
[24] P. Giannozzi *et al.*, J. Phys. Condens. Matter **21**, 395502 (2009).
[25] D. Vanderbilt, Phys. Rev. B **41**, R7892 (1990).
[26] J. P. Perdew, K. Burke, and M. Ernzerhof, Phys. Rev. Lett. **77**, 3865 (1996).
[27] E. Isaev, QHA project, http://qe-forge.org/qha.
[28] Y. Ishikawa, K. Tajima, P. Bloch, and M. Roth, Solid State Commun. **19**, 525 (1976).
[29] Y. N. Zhao, H. L. Han, Y. Yu, W. H. Xue, and T. Gao, Europhys. Lett. **85**, 47 005 (2009).
[30] D. van der Marel, A. Damascelli, K. Schulte, and A. A. Menovsky, Physica (Amsterdam) **244B**, 138 (1998).
[31] A. E. Petrova, V. Krasnorussky, W. Yuhatsz, T. Lograsso, and S. M. Stishov, J. Phys. Conf. Ser. (to be published).
[32] T. Moriya, *Spin Fluctuations in Itinerant Electron Magnetism* (Springer-Verlag, Berlin, 1985).
[33] K. K. Murata and S. Doniach, Phys. Rev. Lett. **29**, 285 (1972).
[34] J. Callaway, Phys. Rev. B **5**, 106 (1972).
[35] K. Makoshi and T. Moriya, J. Phys. Soc. Jpn. **38**, 10 (1975).
[36] P. Mohn and G. Hilscher, Phys. Rev. B **40**, 9126 (1989).